Quantitative MRI for analysis of peritumoral edema in malignant gliomas

Ida Blystad[1,2]*, J. B. Marcel Warntjes[2,3], Örjan Smedby[1,2,4], Peter Lundberg[2,5], Elna-Marie Larsson[2,6☯], Anders Tisell[2,5☯]

1 Department of Radiology and Department of Medical and Health Sciences, Linköping University, Linköping, Sweden, **2** Centre for Medical Image Science and Visualization (CMIV), Linköping University, Linköping, Sweden, **3** Division of Cardiovascular Medicine, Department of Medical and Health Sciences, Linköping University, Linköping, Sweden, **4** School of Technology and Health, KTH Royal Institute of Technology, Stockholm, Sweden, **5** Department of Radiation Physics and Department of Medical and Health Sciences, Linköping University, Linköping, Sweden, **6** Department of Surgical Sciences, Radiology, Uppsala University, Uppsala, Sweden

☯ These authors contributed equally to this work.
* ida.blystad@regionostergotland.se
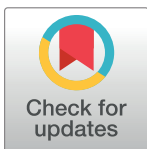
Abstract

Background and purpose

Damage to the blood-brain barrier with subsequent contrast enhancement is a hallmark of glioblastoma. Non-enhancing tumor invasion into the peritumoral edema is, however, not usually visible on conventional magnetic resonance imaging. New quantitative techniques using relaxometry offer additional information about tissue properties. The aim of this study was to evaluate longitudinal relaxation R_1, transverse relaxation R_2, and proton density in the peritumoral edema in a group of patients with malignant glioma before surgery to assess whether relaxometry can detect changes not visible on conventional images.

Methods

In a prospective study, 24 patients with suspected malignant glioma were examined before surgery. A standard MRI protocol was used with the addition of a quantitative MR method (MAGIC), which measured R_1, R_2, and proton density. The diagnosis of malignant glioma was confirmed after biopsy/surgery. In 19 patients synthetic MR images were then created from the MAGIC scan, and ROIs were placed in the peritumoral edema to obtain the quantitative values. Dynamic susceptibility contrast perfusion was used to obtain cerebral blood volume (rCBV) data of the peritumoral edema. Voxel-based statistical analysis was performed using a mixed linear model.

Results

R_1, R_2, and rCBV decrease with increasing distance from the contrast-enhancing part of the tumor. There is a significant increase in R_1 gradient after contrast agent injection (P < .0001). There is a heterogeneous pattern of relaxation values in the peritumoral edema adjacent to the contrast-enhancing part of the tumor.

Competing interests: The authors have read the journal's policy and the authors of this manuscript have the following competing interests: JBMW is part-time employed by Synthetic MR AB. This does not alter our adherence to PLOS ONE policies on sharing data and materials.

Conclusion

Quantitative analysis with relaxometry of peritumoral edema in malignant gliomas detects tissue changes not visualized on conventional MR images. The finding of decreasing R_1 and R_2 means shorter relaxation times closer to the tumor, which could reflect tumor invasion into the peritumoral edema. However, these findings need to be validated in the future.

Introduction

High-grade malignant gliomas are primary brain tumors with an incidence of $\approx 5/100,000$. The prognosis is poor with a median survival of approximately 12–15 months [1]. Magnetic Resonance Imaging (MRI) is extensively used in the diagnostic work-up as well as to monitor treatment. At diagnosis, these tumors show heterogeneous contrast enhancement, often with a necrotic center, and peritumoral edema. Conventional MR imaging relies mainly on visual assessment and the neuroradiologists' ability to recognize patterns. Tumors show contrast enhancement on T1-weighted images (T1W) after gadolinium based contrast agent injection, and the peritumoral edema has a high signal on T2-weighted/fluid attenuation inversion recovery images (T2W/FLAIR). However, it is well known that high-grade malignant gliomas extend beyond the contrast-enhancing border. Diffuse non-enhancing tumor infiltrates into the peritumoral edema [2], and the non-enhancing portions of the tumor have to be considered when assessing patients during follow-up [3]. These diffuse tumor-associated tissue changes are difficult to detect visually on conventional images, and hence the commonly used physiological MR sequences diffusion- and perfusion-weighted imaging (DWI and PWI) may add quantitative information about tumor quality and extension [4]. Diffuse, non-enhancing tumor infiltration into the peritumoral edema can be assessed by a gradient in apparent diffusion coefficient (ADC) values due to the higher cell density [5]and increased cerebral blood volume (CBV) that reflect the tumor-induced neoangiogenesis [6].

High-grade malignant gliomas are aggressive tumors, and they receive aggressive treatment with surgery, chemotherapy, and radiation. This treatment can cause secondary reactions in the non-tumorous brain tissue, resulting in edema and contrast enhancement, i.e. a pattern similar to tumor growth [7,8], which complicates the assessment of follow-up examinations. In these cases with treatment-related changes, such as pseudoprogression and radiation necrosis, conventional MR imaging does not suffice, and quantitative methods, such as DWI, PWI, and MR spectroscopy can add information that can aid in the differentiation between treatment-related changes and tumor recurrence [9–13]. Studies of the peritumoral region with multiparametric pattern analysis to detect the infiltrating parts of the tumor to predict possible locations of tumor recurrence have demonstrated heterogeneity of the peritumoral region [14]. Computational analysis of MR perfusion has provided similar results [15]. However, these methods require advanced mathematical modeling and are not easily implemented in the clinical workflow. So, despite the current arsenal of quantitative/semi-quantitative techniques, follow-up of malignant gliomas remains a challenge because results of the existing methods can be difficult to interpret or to implement in the clinical setting. Hence, there is an interest and a need for development of clinically applicable and robust quantification methods when evaluating patients with brain tumors, in the diagnostic work-up as well as for treatment evaluation and follow-up.

Synthetic MRI [16] is a quantitative MR- sequence (qMRI), acquired in approximately 6 minutes to obtain proton density (PD), longitudinal relaxation rate (R_1) and transverse

relaxation rate (R_2), with correction for B_1- inhomogeneity. From this sequence, synthetic images with a free range of weightings can be produced. The quantitative information of the sequence enables relaxometry measurements of the tissue, which could be a useful addition to conventional imaging in brain tumor investigations.

The purpose of this study was to analyze the relaxation properties of the peritumoral edema in patients with malignant gliomas before surgery, using SyMRI to assess whether relaxometry can detect changes not visible on conventional images of the peritumoral edema.

Materials and methods

Subjects

Twenty-four patients with typical radiological findings suggestive of a high-grade malignant glioma were prospectively included in the study from 2013 to 2016 and examined with MRI before surgery. The diagnosis was confirmed by histopathological analysis after surgery. For patient demographics, see Table 1. Three patients with a histopathological diagnosis of lymphoma, abscess, and primitive neuroectodermal tumor (PNET) were excluded. Two patients were not analyzed due to difficulties in delineating the contrast- enhancing part of the tumor from the peritumoral edema.

The local institutional review board approved the study, and informed written consent was obtained from all patients. Ethical approval was obtained from the Regional Ethical Board Linköping, Sweden, decision number 2011/406-31.

MR acquisition

Images were acquired on a three-tesla (3T) MR scanner (750, GE Medical Systems, Milwaukee, Wisconsin) using a 32-channel phased array head coil according to our clinical protocol for brain tumor investigation, with the addition of the quantitative MR sequence SyMRI MAGIC.

Table 1. Patient demographics.

Patient	Sex	Age	Diagnosis
1	M	63	Anaplastic oligodendroglioma III
2	M	71	Glioblastoma
3	F	58	Glioblastoma
4	M	63	Glioblastoma
5	F	57	Glioblastoma
6	M	65	Glioblastoma
7	F	61	Glioblastoma
8	F	65	Anaplastic oligodendroglioma III
9	M	69	Glioblastoma
10	M	34	Anaplastic oligodendroglioma III
11	M	50	Anaplastic oligodendroglioma III
12	M	79	Glioblastoma
13	M	68	Glioblastoma
14	M	71	Glioblastoma
15	M	65	Gliosarcoma
16	M	46	Glioblastoma
17	M	72	Glioblastoma
18	M	76	Glioblastoma
19	F	45	Glioblastoma

The clinical protocol for brain tumor investigation consists of axial T2WI-FLAIR, T1WI, T2WI, dynamic susceptibility contrast (DSC) perfusion, T1WI-GD, 3D-FSPGR (fast spoiled gradient echo) Gd, and DWI. The sequence parameters for the conventional images used in the study analysis were as follows:

DSC Perfusion gradient-echo EPI (echo planar imaging); axial, field of view (FOV) 220×165, 1 680 slices, voxel size $1.7 \times 1.7 \times 5$ mm (gap 1 mm), TE (echo time) = 29 ms, TR (repetition time) = 1 340 ms, flip angle 60. The perfusion had a 6 s delay before injection with a standard contrast dose of 10 ml gadopentetate dimeglumine (Gd-DTPA, Omniscan, GE Healthcare) 0.5 mmol/ml with an injection rate of 4 ml/s followed by a 15 ml saline flush at an injection rate of 4 ml/s. The total amount of contrast agent was 0.2 ml/kg, with the remaining dose injected after the perfusion series.

T1W spin echo before and after (T1WGd) contrast agent injection: axial, FOV 220×165, 24 slices, voxel size $0.43 \times 0.43 \times 5$ mm (gap 1 mm), TE = 17.7 ms, TR = 2 524 ms, TI (inversion time) = 798 ms.

T2W spin echo PROPELLER: axial, FOV 220×220, 24 slices, voxel size $0.43 \times 0.43 \times 5$ mm (gap 1 mm), TE = 95–97 ms, TR = 3 000 ms.

The quantitative sequence [16], is a multi-slice, multi-echo and multi-saturation delay qMRI technique for simultaneous measurement of R_1, R_2, and PD, with the following parameters in this study.

qMRI MAGIC; axial, FOV 220×180, 24 slices, voxel size $0.43 \times 0.43 \times 5$ mm (gap 1 mm). In total 8 images per slice were measured with TE = 22 ms or 95 ms, TR = 4 000 ms, TI = 170, 670, 1840 or 3840 ms. The scan time was 5:55 minutes, and the qMRI-series was obtained before and after contrast agent injection.

Post-processing and ROI placement

qMRI post-processing. The qMRI sequence yields quantitative maps of R_1, R_2, and PD, which are used for measurements and to create synthetic images matching the conventional images (Fig 1).

The post-processing time of the raw image dataset was approximately 1 minute on an ordinary PC using SyMRI 8 software (SyntheticMR AB, Linköping, Sweden) to create the synthetic images. Relaxation time values (T-values) were obtained from R_1 and R_2 by calculating $T = 1/R$.

Perfusion post-processing. The perfusion data were transferred to a workstation and analyzed with the software NordicICE (version 2.3.12, NordicNeuroLab AS, Bergen, Norway). After motion correction, the realigned perfusion data were used to create whole-brain CBV maps with auto-detected noise threshold and leakage correction. CBV values were normalized against the contralateral hemisphere to obtain relative CBV (rCBV).

ROI analysis. Conventional T2W, T1W, and T1W-Gd images and corresponding synthetic images were transferred to the software MevisLab version 2.7 (MeVis Medical Solutions AG, Bremen, Germany).

A neuroradiologist drew regions of interest (ROIs) for the analysis. The contrast-enhancing border of the tumor was delineated manually (tumor-ROI) in the synthetic T1W image (Fig 2), and a free-hand ROI (edema-ROI) was drawn in the peritumoral edema outside the contrast-enhancing part of the tumor in the synthetic T2W image (Fig 2). ROIs were also placed in synthetic T2W images in the normal appearing white matter (NAWM) adjacent to the tumor edema (NAWM-near-Tumor-ROI), and in the corresponding lobe in the contralateral hemisphere (NAWM-contra-ROI).
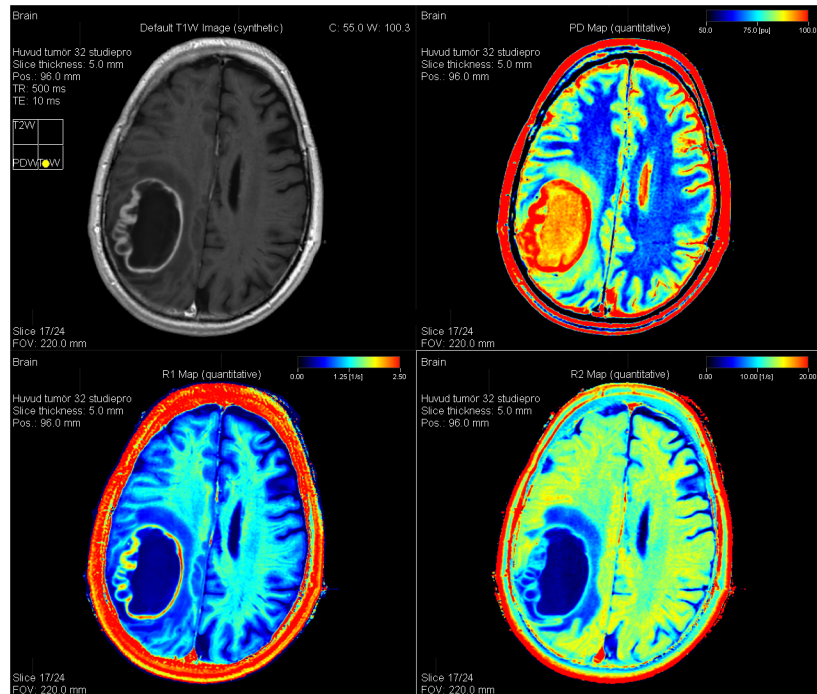
Fig 1. Synthetic images created from the quantitative scan. An example of synthetic T1GdWI (top left), proton density map (top right), R_1 map (bottom left), and R_2 map (bottom right) in a 68-year-old male with a glioblastoma.

https://doi.org/10.1371/journal.pone.0177135.g001
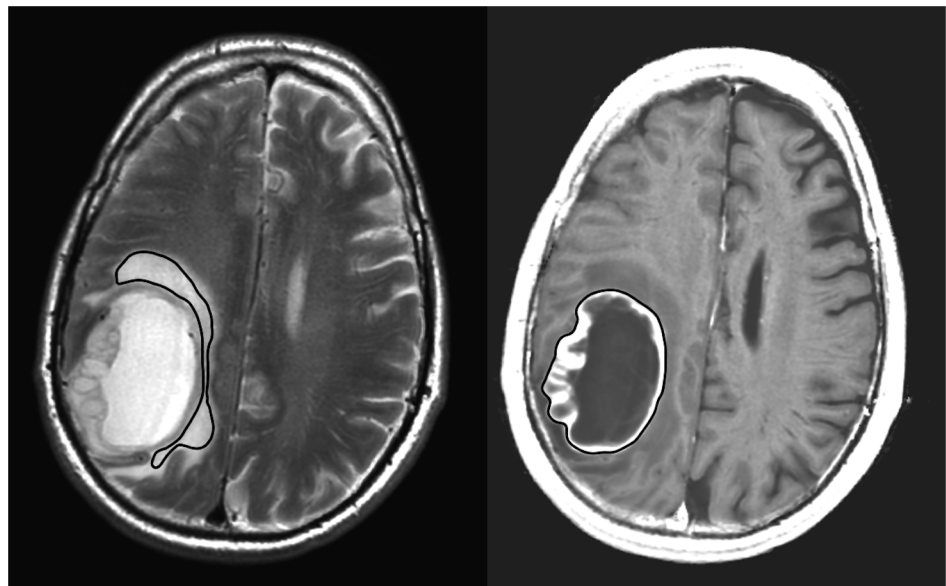
Fig 2. ROIs delineating the peritumoral edema and the contrast-enhancing part of the tumor. A ROI was placed in the peritumoral edema of the synthetic T2WI. The edema ROI was then applied in the qMRI volumes to obtain the quantitative values of R_1, R_2, and proton density. The contrast-enhancing part of the tumor was manually delineated in the synthetic T1GdWI and subtracted to avoid overlap with the edema ROI.

https://doi.org/10.1371/journal.pone.0177135.g002

ROIs delineated in synthetic T2W image volume were directly applied to all images, and to qMRI-maps that were calculated from the same qMRI volume.

However, to apply the tumor-ROI delineated in the qMRI volume post-gadolinium in the qMRI volume pre-gadolinium, a coordinate transformation matrix, M_{GD2pre}, was calculated by image registration of the synthetic T2W-Gd volume to the synthetic T2W volume. The image registration was performed using MevisLab MERIT module, with registration method set to "3D rigid" and similarity measurement to "SSD". To avoid overlap the tumor-ROI was subtracted from the edema-ROI. The inverse transformation matrix M_{GD2pre}^{-1} was used to transform the edema-ROI, NAWM-near-Tumor-ROI and NAWM-contra-ROI to the qMRI-Gd volume.

The edema-ROI, NAWM-near-Tumor-ROI, and NAWM-contra-ROI were also transformed to the CBV map of the perfusion analysis to obtain the rCBV values of the peritumoral edema. This transformation matrix was also calculated using image registration. The synthetic T2W volume was registered to the baseline EPI of the perfusion series using Mevis Lab MERIT module, with the registration method set to 3D rigid transformation and rescaling in each direction and using the normalized cross-correlation (NCC) for similarity measurement.

Statistics

First, the mean values for R_1, R_2, PD and rCBV for each individual ROI were calculated. These values were used to obtain the group mean and standard deviation of each ROI type (edema-ROI, NAWM-near-Tumor-ROI, and NAWM-contra-ROI).

In the edema-ROI, the relationship between the quantitative values and the distance of each individual voxel to the contrast-enhancing part of the tumor was investigated using mixed linear models. The voxel values of the R_1, R_2, PD, and rCBV values were used as dependent variables, the distance to the tumor-ROI was treated as fixed effect, and subject was treated as a random effect.

The difference in slope for R_1 post-Gd compared to the slope in R_1 pre-Gd was analyzed using Student's *t*- test.

All statistical calculations were performed in JMP 8.0 (SAS Inc, Cary, North Carolina).

Results

Measurements of relaxation values in the peritumoral edema revealed a decrease in R_1 and R_2 with increasing distance to the contrast-enhancing border of the tumor, with a significant ($P<0.0001$) gradient from the contrast-enhancing border to the periphery of the edema (Fig 3), with the slope presented as beta-value in the figure. There was a slight increase in PD with increasing distance from the contrast-enhancing part of the tumor. After gadolinium-based contrast agent injection, there was a significant increase in gradient in R_1 ($P < .0001$) (Fig 3).

As seen in Fig 3, there is a heterogeneous pattern of relaxation values within the first 10 mm of the peritumoral edema, possibly reflecting non-enhancing infiltrating tumor as well as peritumoral edema.

rCBV values were higher closer to the tumor, with a gradient from the contrast-enhancing border of the tumor to the periphery of the peritumoral edema (Fig 3).

Fig 4 is an example of synthetic MR images, quantitative maps and graphs of R_1 and R_2 in one of the patients, a 76-year-old man with a glioblastoma. The R_1 graph shows an increase of R_1 after gadolinium based contrast agent injection, with a "tail" extending out into the peritumoral edema. The R_2 graph also depicts a gradient extending into the peritumoral edema.

Table 2 shows the relaxation times, PD, and rCBV of the different tissues measured (edema, NAWM-near-tumor, and NAWM-in-contralateral-hemisphere). Table 3 depicts the slopes
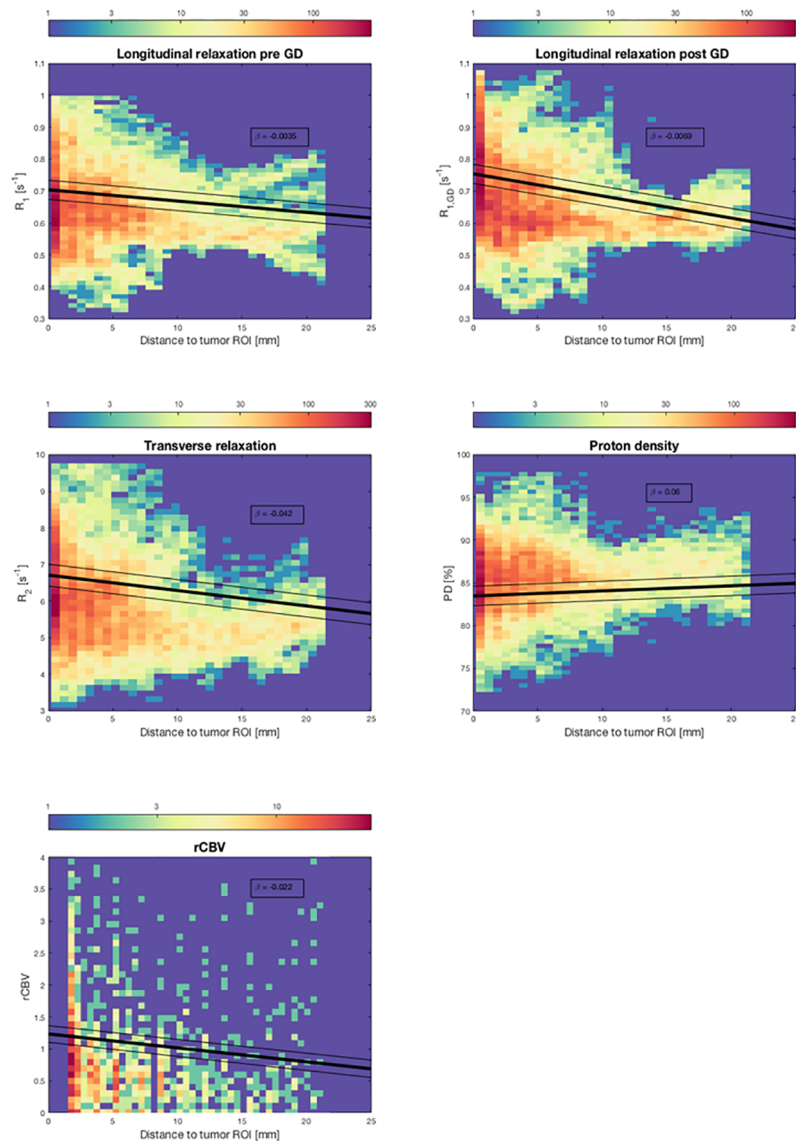
Fig 3. Color histograms of R_1, R_2, proton density and rCBV. Color histograms of R_1, R_2, proton density, and rCBV in the peritumoral edema in relation to distance from the contrast-enhancing part of the tumors of all patients. The thick black lines represent the regression line given by the mixed linear models, with the slope presented as beta value in the figure. The thin black lines represent the confidence intervals. For R_1, R_2, and rCBV, there is a decrease in values with increasing distance from the contrast-enhancing part of the tumor. Proton density has a slight decrease with increasing distance. There is a significant increase in the gradient of the relaxation values after contrast agent injection ($p < 0.001$). The pattern of relaxation values is more heterogeneous closer to the contrast-enhancing part of the tumor.

https://doi.org/10.1371/journal.pone.0177135.g003

with the intercept for the qMRI values and rCBV in relation to distance to the contrast-enhancing part of the tumor.

Discussion

In this study, we found a gradient of relaxation values in the peritumoral edema of malignant gliomas, with shorter relaxation times and a greater heterogeneity in the edema closest to the contrast-enhancing part of the tumor and an increase in the R1 gradient in the edema after
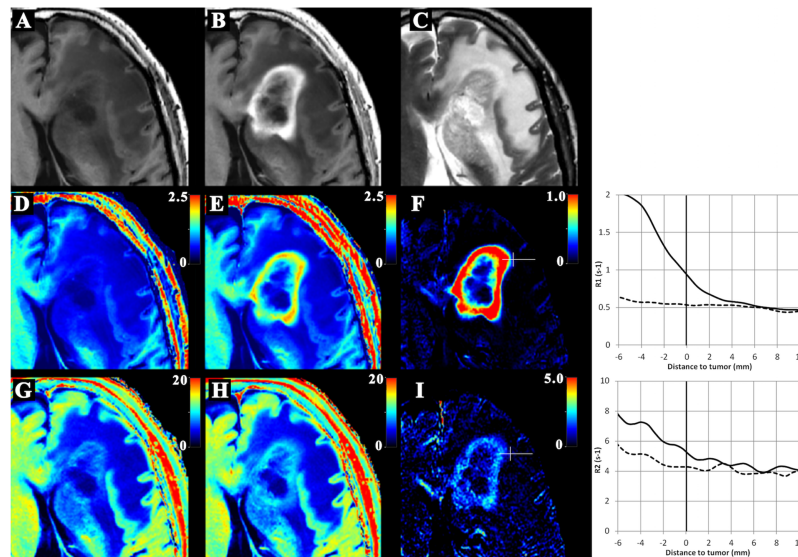
Fig 4. An example of synthetic MRI in one of the patients. Fig 4 is an example of the synthetic and quantitative images of a 76-year-old man with glioblastoma. The top row shows the synthetic images: (A) native T1WI, (B) post-GD T1WI, (C) T2WI post-GD. The center row shows the R1 maps: (D) native R1 map, (E) post-GD R1 map, (F) difference-map of post-GD R1 minus native R1. The bottom row shows the R2 maps: (G) native R2 map, (H) post-GD R2 map, (I) difference-map of post-GD R2 minus native R2. In (F) and (I), a white line is indicated, along which native (dotted line) and post-GD (solid line) data are plotted regarding R1 (top) and R2 (bottom) as a function of the distance to tumor, as shown in the diagrams. The zero distance point is indicated by the small perpendicular line in (F) and (I).

gadolinium based contrast agent injection (Fig 3). These changes could indicate diffuse, non-enhancing tumor infiltration, not visible on conventional MR images.

The diffuse, non-enhancing tumor infiltration is difficult for the radiologist to detect but clinically important for the neurosurgeon and radiotherapy oncologist. During surgery, the aim is radical resection of the tumor [17]. In high-grade gliomas, radical resection is assessed based on the absence of residual contrast enhancement on the immediate post-surgical MRI follow-up performed within 48 hours of surgery. If radical resection is impossible due to tumor location near eloquent regions of the brain, the aim is maximal tumor resection with preservation of brain function. The extent of resection influences the prognosis, and it is known that malignant gliomas extend beyond their contrast-enhancing border with a diffuse, non-enhancing infiltration into the peritumoral edema, which complicates the assessment of the remaining tumor burden [18,19]. These diffuse, non-enhancing tissue changes are not easily detected visually on conventional MR images, but can to some extent be identified with diffusion and perfusion imaging, which correlates with histopathological features of the tumors

Table 2. qMRI values of ROIs: Group mean and SD (N = 19).

Tissue		R1(s^{-1})	R2(s^{-1})	PD(%)	rCBV
		Mean ± SD	Mean ± SD	Mean ± SD	Mean ± SD
Edema-ROI	Pre-Gd	0.69 ± 0.13	6.5 ± 1.3	84 ± 5	
	Post-Gd	0.72 ± 0.14	6.8 ± 1.4	82 ± 6	1.1 ± 0.6
NAWM-near- tumor-ROI	Pre-Gd	1.32 ± 0.11	12.8 ± 0.9	66 ± 3	
	Post-Gd	1.33 ± 0.11	12.9 ± 0.9	66 ± 3	1.2 ± 1.2
NAWM-contra-ROI	Pre-Gd	1.30 ± 0.10	12.5 ± 1.0	66 ± 3	
	Post-Gd	1.31 ± 0.11	12.5 ± 1.1	65 ± 3	-

Table 3. Mixed linear model with qMRI values as dependent variable and distance to tumor as fixed effect.

	Intercept	Beta	t-value	R^2
R_1	0.70	-0.0035***	-36	0.65
R_1GD	0.75	-0.0069***	-53	0.53
R_2	6.71	-0.042***	-41	0.69
R_2GD	6.94	-0.033***	-28	0.63
PD	83.46	0.06***	14	0.50
PDGD	81.39	0.13***	25	0.48
rCBV	1.24	-0.02***	-4	0.2

Table 3 shows the intercept and the slope (beta) of the gradients and the significance levels.

*** = p < .001

[20]. While the diffusion is dependent on the Brownian motion of water and related to e.g. cell density in tumors, relaxation also depends on chemical interaction of the tissues on a microscopic level due to presence of lipids, proteins, macromolecules, and paramagnetic substances [21]. Relaxometry thus adds another type of quantitative information about the tissue.

Non-enhancing tissue changes may affect the outcome in patients with high-grade gliomas [17,22,23], with resection of non-enhancing tumor correlating with longer progression-free survival and overall survival [24].

Previous studies using relaxometry have shown that quantitative T2' is associated with glioma grade, high grade gliomas (WHO III-IV) having a lower T2' value than low-grade gliomas, possibly due to hyper-metabolism [25]. Other studies show that quantitative T1 and T2 mapping during follow-up of treated glioblastomas can provide earlier detection of tumor progression than conventional MR imaging, with a prolongation of T1 and T2 relaxation before the appearance of visible changes in conventional MR-images. The prolongation of T1 possibly results from subtle blood-brain-barrier damage not yet visible on the structural images [26,27]. Ellingson et al [28] used a T2 mapping technique to quantify edema reduction in recurrent glioblastoma treated with bevacizumab, and their result suggested a correlation between posttreatment T2 values and progression free survival.

Thus several studies indicate that measurement of T1 and T2 provides quantitative information about the non-visible tissue changes associated with gliomas, which could help elucidate the nature of these tumors, aid in their diagnostics, and assist treatment planning.

In the present study, we analyzed preoperative MRIs in a cohort of patients with malignant gliomas, currently being monitored during treatment, and future studies will analyze the follow-up examinations to assess treatment-related changes and tumor recurrence using synthetic MRI.

A limitation to this study is the lack of histopathological correlation of the relaxometry measurements of the infiltrated peritumoral edema. However, the findings are in line with other studies showing tumor extension beyond radiological borders in gliomas [29]. Even though the tumor was manually segmented from the peritumoral edema to avoid overlap, the accuracy of the ROI measurements might have been improved by a quantitative sequence with isotropic voxels and thinner slices, a technique that is currently under development.

The R^2 values of the regression lines are relatively low, which indicates that the edema is complex, with several components. This is more evident closer to the contrast-enhancing

border of the tumor, where the relaxation values have a heterogeneous pattern. The heterogeneous pattern could be related to the infiltration of tumor cells into the peritumoral edema.

Conclusion

Quantitative T1 and T2 mapping can detect tissue changes in the peritumoral region that are not visible on conventional MR images. Relaxation values in the peritumoral edema have a heterogeneous pattern within the first 10 mm from the contrast-enhancing portion of the tumor with a gradient in relaxation values from the contrast-enhancing part of the tumor into the peritumoral edema. This may reflect non-visible tumor infiltration into the surrounding tissue, and this information could be useful for the planning of surgery and radiation therapy. The findings, however, need to be further validated.

Supporting information

S1 Dataset. Supporting information file with the quantitative values from the measurements.
(ZIP)

Author Contributions

Conceptualization: IB EML AT PL OS JBMW.

Data curation: IB AT JBMW.

Formal analysis: AT OS.

Funding acquisition: IB PL OS.

Investigation: IB AT JBMW.

Methodology: IB EML AT.

Project administration: IB.

Resources: IB AT PL JBMW.

Software: AT JBMW.

Supervision: EML PL OS.

Validation: AT JBMW.

Visualization: IB AT JBMW.

Writing – original draft: IB.

Writing – review & editing: IB AT EML OS PL JBMW.

References

1. Ostrom QT, Bauchet L, Davis FG, Deltour I, Fisher JL, Langer CE, et al. The epidemiology of glioma in adults: a "state of the science" review. Neuro Oncol [Internet]. 2014; 16(7):896–913. Available from: http://www.ncbi.nlm.nih.gov/pubmed/24842956%5Cnhttp://www.pubmedcentral.nih.gov/articlerender.fcgi?artid=PMC4057143 https://doi.org/10.1093/neuonc/nou087 PMID: 24842956

2. Claes A, Idema AJ, Wesseling P. Diffuse glioma growth: a guerilla war. Acta Neuropathol. 2007 Nov; 114(5):443–58. https://doi.org/10.1007/s00401-007-0293-7 PMID: 17805551

3. Eisele SC, Wen PY, Lee EQ. Assessment of Brain Tumor Response: RANO and Its Offspring. Curr Treat Options Oncol. 2016 Jul; 17(7):35. https://doi.org/10.1007/s11864-016-0413-5 PMID: 27262709

4. Shiroishi MS, Boxerman JL, Pope WB. Physiologic MRI for assessment of response to therapy and prognosis in glioblastoma. Neuro Oncol. 2016 Apr; 18(4):467–78. https://doi.org/10.1093/neuonc/nov179 PMID: 26364321

5. Lemercier P, Paz Maya S, Patrie JT, Flors L, Leiva-Salinas C. Gradient of apparent diffusion coefficient values in peritumoral edema helps in differentiation of glioblastoma from solitary metastatic lesions. AJRAmerican J Roentgenol. 2014 Jul; 203(1):163–9.

6. Blasel S, Jurcoane A, Franz K, Morawe G, Pellikan S, Hattingen E. Elevated peritumoural rCBV values as a mean to differentiate metastases from high-grade gliomas. Acta Neurochir (Wien). 2010 Nov; 152 (11):1893–9.

7. Brandsma D, Stalpers L, Taal W, Sminia P, van den Bent MJ. Clinical features, mechanisms, and management of pseudoprogression in malignant gliomas. The LancetOncology. 2008 May; 9(5):453–61.

8. Hygino da Cruz LC Jr, Rodriguez I, Domingues RC, Gasparetto EL, Sorensen AG. Pseudoprogression and pseudoresponse: imaging challenges in the assessment of posttreatment glioma. AJNRAmerican J Neuroradiol. 2011 Dec; 32(11):1978–85.

9. Young RJ, Gupta A, Shah AD, Graber JJ, Chan TA, Zhang Z, et al. MRI perfusion in determining pseudoprogression in patients with glioblastoma. Clin Imaging. 2013; 37(1):41–9. https://doi.org/10.1016/j.clinimag.2012.02.016 PMID: 23151413

10. Boxerman JL, Ellingson BM, Jeyapalan S, Elinzano H, Harris RJ, Rogg JM, et al. Longitudinal DSC-MRI for Distinguishing Tumor Recurrence From Pseudoprogression in Patients With a High-grade Glioma. Am J Clin Oncol. 2014 Nov 26;

11. Prager AJ, Martinez N, Beal K, Omuro A, Zhang Z, Young RJ. Diffusion and perfusion MRI to differentiate treatment-related changes including pseudoprogression from recurrent tumors in high-grade gliomas with histopathologic evidence. AJNRAmerican J Neuroradiol. 2015 May; 36(5):877–85.

12. Wang S, Martinez-Lage M, Sakai Y, Chawla S, Kim SG, Alonso-Basanta M, et al. Differentiating Tumor Progression from Pseudoprogression in Patients with Glioblastomas Using Diffusion Tensor Imaging and Dynamic Susceptibility Contrast MRI. AJNRAmerican J Neuroradiol. 2016 Jan; 37(1):28–36.

13. Zhang H, Ma L, Wang Q, Zheng X, Wu C, Xu BN. Role of magnetic resonance spectroscopy for the differentiation of recurrent glioma from radiation necrosis: a systematic review and meta-analysis. Eur J Radiol. 2014 Dec; 83(12):2181–9. https://doi.org/10.1016/j.ejrad.2014.09.018 PMID: 25452098

14. Akbari H, Macyszyn L, Da X, Bilello M, Wolf RL, Martinez-Lage M, et al. Imaging Surrogates of Infiltration Obtained Via Multiparametric Imaging Pattern Analysis Predict Subsequent Location of Recurrence of Glioblastoma. Neurosurgery. 2016 Apr; 78(4):572–80. https://doi.org/10.1227/NEU.0000000000001202 PMID: 26813856

15. Akbari H, Macyszyn L, Da X, Wolf RL, Bilello M, Verma R, et al. Pattern analysis of dynamic susceptibility contrast-enhanced MR imaging demonstrates peritumoral tissue heterogeneity. Radiology. 2014 Nov; 273(2):502–10. https://doi.org/10.1148/radiol.14132458 PMID: 24955928

16. Warntjes JB, Leinhard OD, West J, Lundberg P. Rapid magnetic resonance quantification on the brain: Optimization for clinical usage. Magn Reson Med. 2008 Aug; 60(2):320–9. https://doi.org/10.1002/mrm.21635 PMID: 18666127

17. Grabowski MM, Recinos PF, Nowacki AS, Schroeder JL, Angelov L, Barnett GH, et al. Residual tumor volume versus extent of resection: predictors of survival after surgery for glioblastoma. J Neurosurg. 2014 Nov; 121(5):1115–23. https://doi.org/10.3171/2014.7.JNS132449 PMID: 25192475

18. Chaichana KL, Jusue-Torres I, Navarro-Ramirez R, Raza SM, Pascual-Gallego M, Ibrahim A, et al. Establishing percent resection and residual volume thresholds affecting survival and recurrence for patients with newly diagnosed intracranial glioblastoma. Neuro Oncol. 2014 Jan; 16(1):113–22. https://doi.org/10.1093/neuonc/not137 PMID: 24285550

19. Lemee JM, Clavreul A, Aubry M, Com E, de Tayrac M, Eliat PA, et al. Characterizing the peritumoral brain zone in glioblastoma: a multidisciplinary analysis. J Neurooncol. 2015 Mar; 122(1):53–61. https://doi.org/10.1007/s11060-014-1695-8 PMID: 25559687

20. Barajas RF Jr, Phillips JJ, Parvataneni R, Molinaro A, Essock-Burns E, Bourne G, et al. Regional variation in histopathologic features of tumor specimens from treatment-naive glioblastoma correlates with anatomic and physiologic MR Imaging. Neuro Oncol. 2012 Jul; 14(7):942–54. https://doi.org/10.1093/neuonc/nos128 PMID: 22711606

21. Deoni SCL. Quantitative Relaxometry of the Brain. [cited 2017 Mar 10]; https://www.ncbi.nlm.nih.gov/pmc/articles/PMC3613135/pdf/nihms294764.pdf

22. Jain R, Poisson LM, Gutman D, Scarpace L, Hwang SN, Holder CA, et al. Outcome prediction in patients with glioblastoma by using imaging, clinical, and genomic biomarkers: focus on the nonenhancing component of the tumor. Radiology. 2014 Aug; 272(2):484–93. https://doi.org/10.1148/radiol.14131691 PMID: 24646147

23. Yan JL, van der Hoorn A, Larkin TJ, Boonzaier NR, Matys T, Price SJ. Extent of resection of peritumoral diffusion tensor imaging-detected abnormality as a predictor of survival in adult glioblastoma patients. J Neurosurg. 2016 Apr 8;1–8.

24. Li YM, Suki D, Hess K, Sawaya R. The influence of maximum safe resection of glioblastoma on survival in 1229 patients: Can we do better than gross-total resection? J Neurosurg. 2016 Apr; 124(4):977–88. https://doi.org/10.3171/2015.5.JNS142087 PMID: 26495941

25. Saitta L, Heese O, Forster AF, Matschke J, Siemonsen S, Castellan L, et al. Signal intensity in T2' magnetic resonance imaging is related to brain glioma grade. Eur Radiol. 2011 May; 21(5):1068–76. https://doi.org/10.1007/s00330-010-2004-3 PMID: 21069342

26. Hattingen E, Jurcoane A, Daneshvar K, Pilatus U, Mittelbronn M, Steinbach JP, et al. Quantitative T2 mapping of recurrent glioblastoma under bevacizumab improves monitoring for non-enhancing tumor progression and predicts overall survival. Neuro Oncol. 2013 Oct; 15(10):1395–404. https://doi.org/10.1093/neuonc/not105 PMID: 23925453

27. Lescher S, Jurcoane A, Veit A, Bahr O, Deichmann R, Hattingen E. Quantitative T1 and T2 mapping in recurrent glioblastomas under bevacizumab: earlier detection of tumor progression compared to conventional MRI. Neuroradiology. 2014 Oct 7;

28. Ellingson BM, Cloughesy TF, Lai A, Nghiemphu PL, Lalezari S, Zaw T, et al. Quantification of edema reduction using differential quantitative T2 (DQT2) relaxometry mapping in recurrent glioblastoma treated with bevacizumab. J Neurooncol. 2012 Jan; 106(1):111–9. https://doi.org/10.1007/s11060-011-0638-x PMID: 21706273

29. Zetterling M, Roodakker KR, Berntsson SG, Edqvist PH, Latini F, Landtblom AM, et al. Extension of diffuse low-grade gliomas beyond radiological borders as shown by the coregistration of histopathological and magnetic resonance imaging data. J Neurosurg. 2016 Feb 26;1–12.